Revue des Composites et des Matériaux Avancés-Journal of Composite and Advanced Materials
Vol. 36, No. 3, June, 2026, pp. 563-569
Journal homepage: http://iieta.org/journals/rcma

Temperature Dependence of Elastic Modulus for Porous Superconducting Material YBCO

Hamdi Farah

Instrumentation Laboratory, Department of Electronics, Faculty of Electrical Engineering, University of Science and Technology Houari Boumediene (USTHB), Algiers 16111, Algeria

Corresponding Author Email: f_7amdi@yahoo.fr

https://doi.org/10.18280/rcma.360310

Received: 22 April 2026
Revised: 15 June 2026
Accepted: 24 June 2026
Available online: 30 June 2026

Keywords:
elastic constants, analytical model, porosity, temperature, porous superconducting materials, acoustic signature, ultrasonic wave velocity

ABSTRACT

Elastic constants are essential for understanding material behavior, particularly in superconducting materials. This study focuses on how temperature affects the elastic constants and ultrasonic wave velocity of a superconducting material in both non-porous and porous states. Additionally, temperature and porosity are treated as independent variables within an appropriate temperature range. This work numerically investigates the impact of temperature and porosity on the elastic properties of the porous superconducting material $YBa_2Cu_3O_{7-x}$ (YBCO or Y123). The study employs a model-based approach, utilizing an empirical model of ultrasonic wave velocities as a function of temperature and porosity, which is validated against previously published experimental data on porous superconducting materials. A new rational model is proposed, where each parameter has a distinct physical meaning, to describe the longitudinal wave velocity (V_L), transverse wave velocity (V_T), and Rayleigh wave velocity (V_R) as functions of temperature across a range of 5 to 300 K and porosity rates from 1.1% to 37.3%. The acoustic signature of the material, $V(z)$, is simulated using an acoustic microscope at a working frequency of 570 MHz and analyzed through the reflection coefficient $R(\theta)$. Fast Fourier Transform (FFT) analysis of the $V(z)$ curves facilitates the extraction of V_R. Consequently, the elastic moduli—specifically, Young's modulus (E), shear modulus (G), and bulk modulus (K)—are determined across the entire temperature range of 5 to 300 K for various porosity levels, yielding a comprehensive description of the elastic behavior of porous YBCO superconductors. Comparisons with experimental data from previous studies indicate that the proposed model accurately reproduces reference ultrasonic velocities and the derived elastic moduli across all considered temperature and porosity ranges. The primary contribution of this work is the development of a unified temperature-porosity model that can jointly predict the velocities of ultrasonic waves and the elastic moduli (E, G, K) of YBCO superconducting materials, spanning from extremely low to high temperatures under different porosity conditions. These findings enhance the understanding of the behavior and performance of porous YBCO superconducting materials across a wide temperature range, as influenced by temperature and porosity, and provide a new methodological framework for the non-destructive characterization of their elastic properties using acoustic microscope technique.

1. INTRODUCTION

The ultrasonic wave's velocity in a solid depends on the density of the material and its elasticity. The elastic moduli can be obtained from measurements of the propagation of longitudinal and transverse waves along specific crystallographic directions, giving direct information on the fundamental mechanical properties. Therefore, the measurement and modelling of these moduli are of great importance in materials research, especially in the field of ceramic superconductors. They find application in a wide range of technologies including sensors, magnets and power transmission systems within the medical, aerospace and energy industries [1-4]. In addition to these applications, superconducting materials are of considerable fundamental interest because the microscopic mechanisms that depend on high-temperature superconductivity are still only partially understood, and the precise characterization of their mechanical and elastic behavior can provide indirect information on the structural changes that accompany the superconducting transition effect of temperature on ultrasound velocity.

The main physical factor determining the propagation of ultrasonic waves in superconducting materials is temperature. Variations in the dynamics of the crystal lattice and in electron-phonon coupling occur in the vicinity of and below the critical temperature (Tc ≈ 90 K for YBCO). These variations have a direct effect on the velocities of longitudinal

(V_L) and transverse waves (V_T) and, accordingly, on the elastic moduli [5-7]. The temperature dependency of several models of superconducting and ceramic materials has been theoretically investigated. The ultrasonic wave velocity is known to depend on temperature in a wide temperature range, from very low temperatures to ambient and high temperatures. This temperature effect, spanning from very low cryogenic temperatures to ambient and elevated temperatures, has been the subject of extensive theoretical and experimental effort over the last several decades. These efforts have aimed to develop trustworthy predictive models. These developments have substantially increased our understanding of the role of thermal effects in the ultrasonic and elastic moduli of superconducting ceramics and provide a good basis for future improvements in the effect of porosity on ultrasonic velocity [8, 9].

In addition to temperature, porosity is the second main factor affecting the propagation of ultrasonic waves. The development of porous ceramic manufacturing methods is largely due to advances in nondestructive testing (NDT) [10]. Acoustic microscopy has been successfully used on porous ceramics in general [11], particularly to characterize the relationship between porosity, ultrasonic wave velocity, and elastic moduli [12, 13]. These studies have proven that an increase in porosity is often accompanied by a measurable decrease in wave velocity and elastic stiffness. Porosity was found to be an important parameter in the elastic characterization of porous materials in these studies. However, most studies consider only the porosity at a fixed or ambient temperature.

Therefore, we characterized the YBCO superconducting material ($YBa_2Cu_3O_{7-x}$) in porous and non-porous forms using acoustic microscopy. The major purpose of this study was to build a model of the simultaneous evolution of longitudinal (V_L), transverse (V_T), and Rayleigh (V_R) wave velocities as a function of temperature and porosity. First, the acoustic signature of the material, $V(z)$, was simulated as a function of temperature and porosity. This signature is due to the reflection coefficient, each corresponding to a given propagation mode at the sample surface. The $V(z)$ response, once simulated, was evaluated using FFT, which is a signal processing technique that allows the determination of the distinct elastic moduli of the porous superconducting material [12]. This methodology for determining these moduli is also described.

The preceding literature review can be classified into two broad research directions: one related to the temperature dependency of velocities, and the other related to the ultrasonic wave velocity in superconducting materials. The other concerns the dependence of these same velocities on porosity, a subject that is usually researched in ceramics at a given temperature. It is therefore expected that these two factors interact in real porous superconductors under different thermal conditions. However, no common theoretical model can predict the joint and interdependent dependence of the ultrasonic wave velocities in superconductors on temperature and porosity. This is a major gap in the current knowledge because it is not realistic to believe that temperature and porosity work independently.

This study closes this gap by offering a porosity and temperature-dependent rational model of ultrasonic wave velocity, linking the previously described temperature and porosity dependence techniques.

2. ANALYTICAL PROCEDURE

The nature and structure of the material [12-14] are related to the values of elastic moduli that characterize it, such as Young's (E), Shear (G), and Bulk (K) moduli. These moduli are calculated using the following equations:

$$E = \rho V_T^2 \frac{3V_L^2 - 4V_T^2}{V_L^2 - V_T^2} \quad (1)$$

$$G = \rho V_T^2 \quad (2)$$

$$K = \rho \left(V_L^2 - \frac{4}{3}V_T^2\right) \quad (3)$$

where, ρ is the material density, V_T and V_L are the transverse and longitudinal velocities.

The well-known Sheppard and Wilson model is used to simulate the acoustic signature of materials [15]:

$$V(z) = \int P^2(\theta)\, \mathrm{R}(\theta)\, \sin\theta\, \cos\theta\, \exp(2\mathrm{ikz}\cos\theta)\mathrm{d}\theta \quad (4)$$

where, k is the wave number in the coupling liquid, $P(\theta)$ is the lens function pupil, z is the defocusing of the sensor concerning the focal length, θ is the angle between the wave K vector and the lens axis, and $R(\theta)$ [15, 16].

Note that this signature is related to the reflection coefficient $R(\theta)$ by the following relationship:

$$R(\theta) = \frac{(Z_L \mathrm{Cos}^2 2\theta_T + Z_T \mathrm{Sin}^2 2\theta_T - \frac{\rho_{Liq} V_{Liq}}{\mathrm{Cos}\,\theta})}{(Z_L \mathrm{Cos}^2 2\theta_T + Z_T \mathrm{Sin}^2 2\theta_T + \frac{\rho_{Liq} V_{Liq}}{\mathrm{Cos}\,\theta})} \quad (5)$$

where, Z_L, Z_T are the longitudinal and transverse impedance, respectively; V_{Liq} is the liquid velocity; ρ_{Liq} is the liquid density.

The acoustic signature, $V(z)$ curve, comprises pseudo-periodic, ΔZ, signals, where we can reveal information about the acoustic surface wave thanks to the periodicity of the interferences. From this period, we calculate the Rayleigh mode's propagation velocity, V_R, in (m/s) by the use of the following relation [12]:

$$V_R = \frac{V_{Liq}}{(1 - (\frac{V_{Liq}}{2 f \Delta Z})^2)^{1/2}} \quad (6)$$

where, V_{Liq} is the velocity of the liquid, and f is the working frequency.

We note that to determine the period ΔZ, we apply the spectral method FFT:

$$\Delta Z = \frac{V_{Liq}}{2f(1 - Cos\,\theta_R)} \quad (7)$$

After spectral analysis by FFT of the signal $V(z)$, we can also calculate the elastic constants of the materials by this procedure.

In the literature [17, 18], for porous materials, the wave velocities change with the change of the porosity rate, p,

through empirical relationships formulated as follows:

$$V_T = V_{T0}(1 - a_1 p)^n \quad (8)$$

$$V_L = V_{L0}(1 - b_1 p)^m \quad (9)$$

$$\rho = \rho_0(1 - p) \quad (10)$$

where, a_1, b_1, n, m are fitting parameters and a material with no pores is indicated by the subscript "0".

Thus, there is a vast amount of literature on the research of the porosity effect on ultrasonic wave velocities, both in experiment and theory [19, 20].

On the other hand, the empirical relationships most frequently used by Vasudev for temperature-dependent ultrasonic wave velocities are [21, 22]:

$$V = V_0 - bT \quad (11)$$

$$V = V_0 - BT \exp(-\frac{T_0}{T}) \quad (12)$$

where, V_0 is the ultrasonic wave velocity at absolute zero and b, B, and T_0 are constants.

3. RESULTS AND DISCUSSION

3.1 Temperature effect on the superconducting material YBCO

The acoustic technique was used in our research, as it relies on modeling the acoustic signature (Eq. (4)), which is related to the reflection coefficient. We developed a program on the computer to determine the acoustic signature based on the calculated reflection coefficient using measured ultrasound velocities (V_L and V_T) for different temperature values in the nonporous and porous cases. Because this study relies on a modeling approach, the V_L and V_T of the superconducting material YBCO as a function of temperature and porosity were obtained from the NIST Structural Ceramics Database via previous studies [23-28].

As simulated conditions, we used a working frequency of 570 MHz (high frequency) to allow the propagation of the ultrasonic waves in the solid. As a coupling fluid, we used water.

Table 1. Ultrasonic wave velocities of YBCO parameters at 300 K

V_{L0}^{exp}, m/s [24]	V_{L0}^{mod}, m/s	a_1	n
5560	5650	2.08	0.340
V_{T0}^{exp}, m/s [24]	V_{T0}^{mod}, m/s	b_1	m
3130	3130	2.10	0.225

Note: The parameters a_1, b_1, n, and m are the nonlinear acoustic coefficients (see Eqs. (8)-(10) for their definitions). Superscripts "exp" and "mod" denote experimental and model values, respectively; and a material with no pores is indicated by the subscript "0".

Masi et al. [28] reported experimental values of ultrasonic velocities (V_L and V_T) of YBCO with porosities ranging from 1.1% to 37.3%. Table 1 and Table 2 list all the model-fitting parameters, before the reflection coefficient is determined, of Eqs. (8) and (9) to the experimental data of the V_T and V_L values, which constitutes the first stage.

Table 2 shows a remarkable agreement between the simulated velocity of porous YBCO and the experimental data.

Table 2. Ultrasonic wave velocities of porous YBCO parameters at 300 K

p, %	21	37.3
V_L^{exp} m/s [28]	4550	3320
V_L^{mod} m/s [28]	4648	3398
E_{VL} %	2.15	2.35
V_T^{exp} m/s [28]	2630	2020
V_T^{mod} m/s [28]	2746	2218
E_{VT} %	4.41	9.8

Note: E_{VL}, E_{VT}: Relative Absolute Error (%) for V_L and V_T, respectively.

Tables 3 and 4 show the results confirming the accuracy and reliability of the proposed model for the non-destructive characterization of YBCO-based superconducting devices.

Table 3. Longitudinal velocity (V_L) of YBCO parameters as a function of temperature

T, K	V_L^{mod}, m/s	V_L^{exp}, m/s [23]	E_L, m/s	E_L, %
18	4300.8	4300	0.8	0.019
124	2275.3	2274.5	0.8	0.019
300	4235.5	4242	6.5	0.153

Note: T represents temperature; superscripts "exp" and "mod" denote experimental and model values, respectively. ΔE_L, E_L: Absolute Error (m/s), Absolute Relative Error (%) for longitudinal velocity, respectively.

Table 4. Transverse velocity (V_T) of YBCO parameters as a function of temperature

T, K	V_T^{mod}, m/s	V_T^{exp}, m/s [23]	E_T, m/s	E_T, %
18	2657.1	2660.8	3.7	0.139
124	2636	2636	0	0
300	2599	2594.9	4.1	0.158

Note: T represents temperature; superscripts "exp" and "mod" denote experimental and model values, respectively. ΔE_T, E_T: Absolute Error (m/s), Absolute Relative Error (%) for transversal velocity, respectively.

Furthermore, the temperature dependence of the ultrasonic velocity exhibits very low and stable errors, all below 0.16%, which confirms the validity of the linear thermal model (Eq. (11)).

3.2 Acoustic signature $V(z)$ and its treatment by Fast Fourier Transform

Figure 1 shows $V(z)$ curves modeling for various temperature values (18 K, 124 K, and 300 K). Depending on the temperature, the period of the pseudo-oscillations decreases; some acoustic signature curves were obtained, indicating a change in the velocities of the propagating modes in the examined superconducting material.

We can determine the velocities of surface and volume wave propagation by processing the $V(z)$ curves using the FFT. Moreover, the spectra show that this analysis makes it possible to characterize the surface mode, which is the Rayleigh mode. This mode aligns with Rayleigh's critical angle and provides the V_R as a result. It can be seen that this velocity decreases with increasing temperature (Figure 1).

Figure 2 illustrates the effect of temperature and porosity on the V_R.

Moreover, the V_R decreases with or without porosity as the temperature increases.

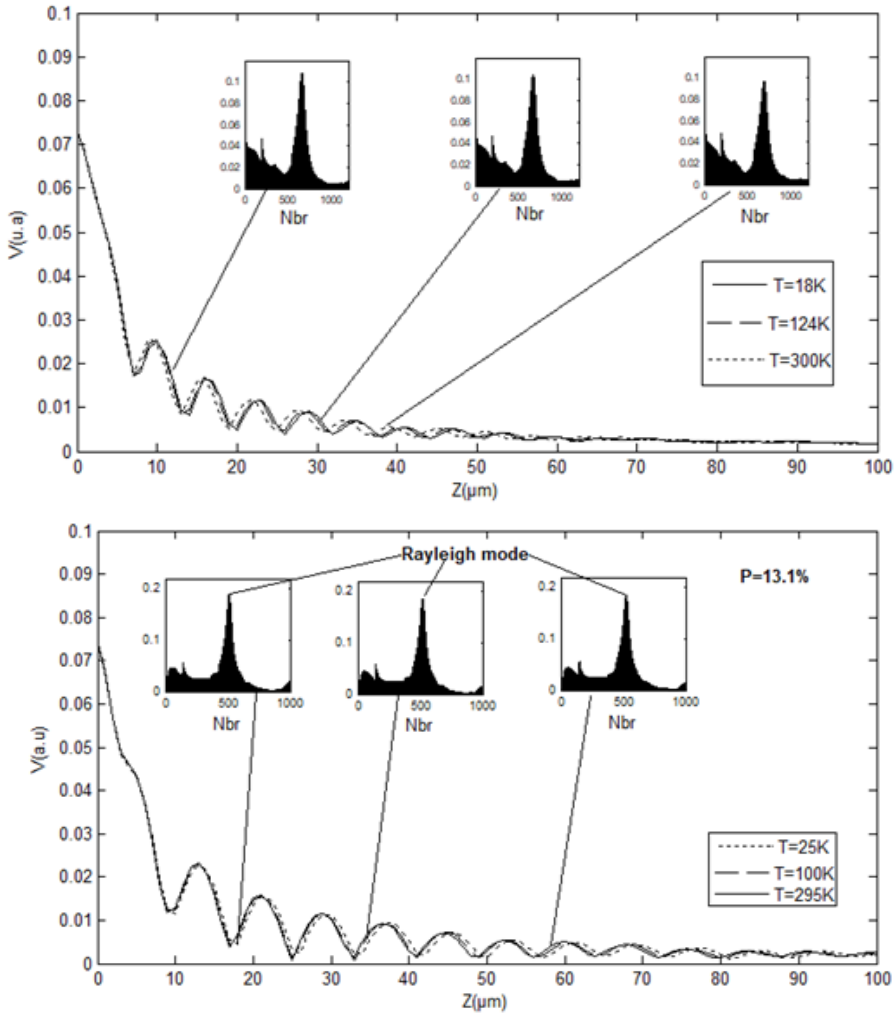

Figure 1. The acoustic signature with Fast Fourier Transform (FFT) analysis of $V(z)$ YBCO for different temperature values at p = 0% and p = 13.1%

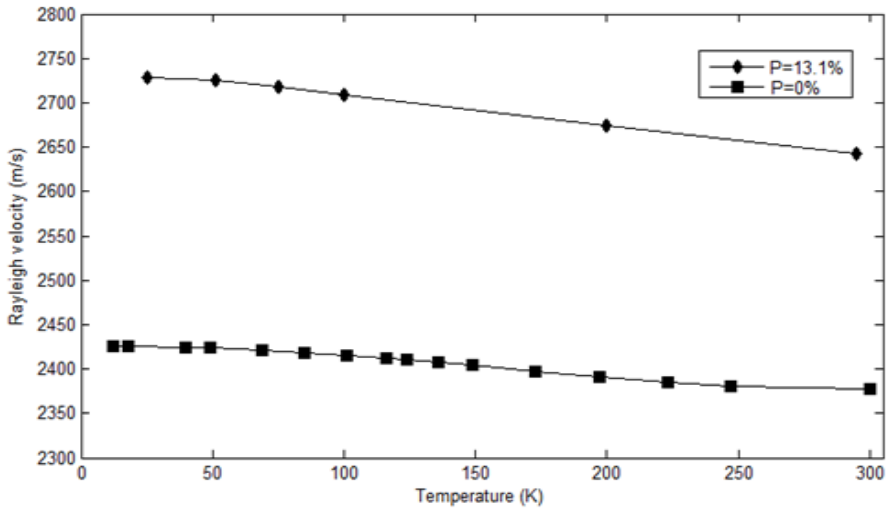

Figure 2. Variation of the Rayleigh wave velocity (V_R) depending on the temperature for p = 0% and p = 13.1%

3.3 Identification of the elastic properties

The velocities of the propagating modes and the elasticity moduli dependent on temperature for nonporous and porous states in the investigated superconducting material were calculated from $V(z)$ curves.

3.3.1 Temperature dependence

Table 5 shows that the observed behavior of the elasticity coefficients is very similar to the previously observed behavior of the ultrasonic wave velocities (V_L and V_T).

Furthermore, the error is minimal at 124 K, slightly larger at 18 K, and maximum at 300 K. This result confirms that the point of maximum deflection is consistently located at room

temperature and not near the superconducting transition temperature (Tc).

Table 5. The elastic moduli as a function of temperature (p = 0)

T, K	E_{EXP}, GPa [23]	E_{mod}	G_{EXP}, GPa	G_{mod}	K_{EXP}, GPa	K_{mod}
18	95.70	95.87	39.41	39.56	51.66	51.64
124	94.52	94.50	39.65	39.78	51.20	51.06
300	92.20	91.91	38.4	38.31	-	51.14

Note: Temperature (T), Young's modulus (E), shear modulus (G), and bulk modulus (K); EXP = experimental, and mod = model.

Table 6 shows that the relative error remains below 0.32% across all elastic moduli (E, G, and K) as a function of temperature of YBCO superconducting material, confirming the model's excellent accuracy. The largest error consistently appears at 300 K for all three moduli, suggesting that the discrepancy between model and experiment tends to increase slightly with temperature within this range.

The mean absolute error (MAE) for the elastic E, G, and K moduli never exceeds 0.2%. These error levels are significantly lower than the 0.5% threshold generally considered excellent for this type of modeling, confirming the robustness of the linear thermal model for describing the evolution of the elastic properties of Y123 as a function of temperature.

Table 6. Errors calculation for elastic moduli

T, K	E_E, %	E_G, %	E_K, %
18	0.177	0.279	0.213
124	0.016	0	0.076
300	0.314	0.315	0.296
Mean absolute error (MAE)	0.168	0.198	0.195

Note: E_E, E_G, E_K: Relative Absolute Error (%) for E, G and K moduli, respectively.

3.3.2 Porosity dependence

Figures 3 and 4 show the evolution of Young's bulk and shear modulus depending on temperature for different porosity rates.

It is observed that the elastic constants decrease with increasing temperature, and this is in accord with those obtained in the experimental measurements (see Figure 3) [23-29]; for example, at p= 13.1% for T = 25 K, Young's modulus E = 121.2 GPa and for T = 295 K, E = 113.69 GPa. It is noted that with the presence or absence of porosity, the temperature increase causes these parameters to decrease (Table 7).

Table 8 shows that the MAE, calculated from the porosity value, is very low for the moduli E (0.030) and G (0.010), confirming the excellent accuracy of the modeling.

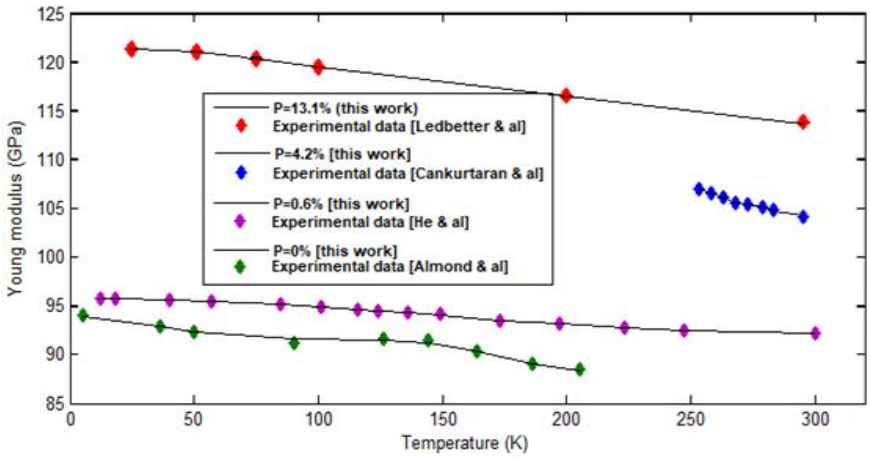

Figure 3. Comparison between experimental and calculated values of Young's modulus (E) depending on temperature with porosity: p = 0, p = 4.2%, p = 6%, p = 13.1%, respectively

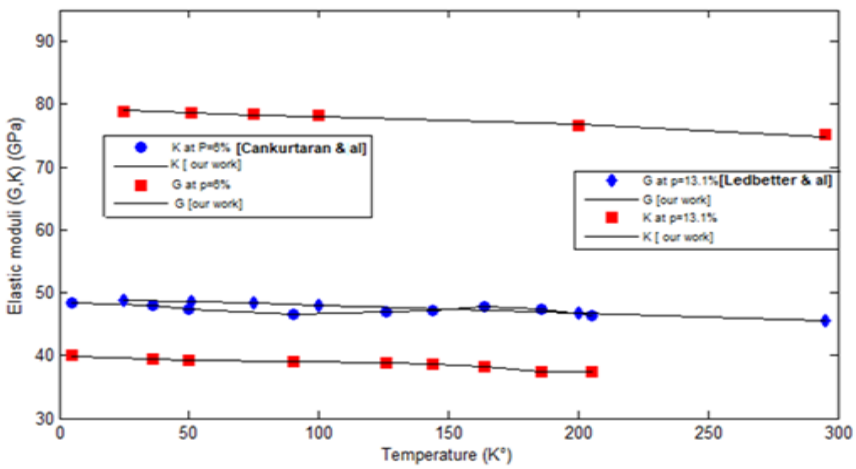

Figure 4. Comparison between calculated and experimental: Shear (G) and bulk (K) moduli dependent on temperature with two porosities: p = 6% and p = 13.1%

Table 7. The elastic moduli as a function of porosity (T = 295 K)

p, %	E_{EXP}	E_{mod}, GPa	G_{EXP}, GPa	G_{mod}	K_{EXP}, GPa	K_{mod}
4.2 [25]	104.20	104.25	44.80	44.81	51.60	51.60
13.1 [29]	113.70	113.69	45.60	45.59	75.10	74.81

Note: Temperature (T), Young's modulus (E), shear modulus (G), and bulk modulus (K); EXP = experimental, and mod = model.

Table 8. Error calculation for elastic moduli at T = 295 K

p, %	E_E, %	E_G, %	E_K, %
4.2	0.048	0.022	0
13.1	0.009	0.022	0.386
MAE	0.030	0.010	0.145

Note: E_E, E_G, E_K: Relative Absolute Error (%) for E, G and K moduli, respectively.

4. CONCLUSIONS

In summary, this study proposed a new numerical approach to characterize porous and non-porous YBCO superconducting materials by the acoustic microscopy technique. An ultrasonic wave velocity model, dependent on temperature and porosity, was developed by modeling the acoustic microscopy technique. The acoustic signature of the material $V(z)$ obtained by integration of the reflection coefficient was then analyzed by FFT, as a function of the temperature and porosity of the polycrystalline superconducting YBCO materials, in order to extract the V_R. The set of elastic moduli (E, G, K) was then analytically deduced from these velocities as functions of temperature and different porosity rates. The systematic comparison of the simulated results with the experimental data available in the literature reveals satisfactory agreement, with relative deviations less than 0.2%, thus confirming the physical relevance and quantitative reliability of the proposed model.

We also determined the elastic moduli (E, G, K) as a function of temperature (from 5 to 300 K) and porosity (from 1.1% to 37.3%). Comparison with available experimental data shows good overall agreement, with the MAE and the maximum deviation remaining within an acceptable range across all temperature and porosity intervals considered. This confirms that the proposed model is reliable for describing the elastic behavior of porous superconducting materials.

5. PERSPECTIVES

It is imperative to emphasize the numerous constraints of this investigation. At first, the superconducting transition region was not examined because of an absence of experimental data in the scientific literature for this specific temperature range. Secondly, the model validation depends entirely on experimental data previously published, rather than on direct measurements that were conducted within the context of this study. This may limit the model's evaluation under conditions not addressed in existing research. Third, the model's behavior beyond these conditions has not been verified; the porosity range considered in this study is restricted to values below 50%.

Several potential avenues exist for expanding this research. Subject to the future availability of dedicated experimental data in this temperature range, the model's extension to the superconducting Tc remains a substantial possibility. In addition, the proposed method could be extended to other families of porous superconducting materials in order to evaluate the generality of the temperature-porosity model beyond the YBCO system. Lastly, the proposed methodology's validity limits could be established by expanding the study to higher porosity rates.

REFERENCES

[1] Xiao, G., Cieplak, M.Z., Musser, D., Gavrin, A., Streitz, F.H., Chien, C.L., Rhyne, J.J., Gotaas, J.A. (1988). Significance of plane versus chain sites in high-temperature oxide superconductors. Nature, 332: 238-240. https://doi.org/10.1038/332238a0

[2] Ekicibil, A., Karadağ, F., Çetin, S.K., Ayaş, A.O., Akça, G., Akyol, M., Kaya, D. (2022). Transport properties of superconducting materials. In Superconducting Materials: Fundamentals, Synthesis and Applications, pp. 29-60. https://doi.org/10.1007/978-981-19-1211-5_2

[3] Yakhmi, J.V. (2021). Superconducting Materials and Their Applications: An Interdisciplinary Approach. Institute of Physics Publishing.

[4] Kovalev, K., Poltavets, V., Kolchanova, I. (2019). Superconducting technologies for renewable energy. E3S Web of Conferences, 124: 01043. https://doi.org/10.1051/e3sconf/201912401043

[5] Ledbetter, H.M., Austin, M.W., Kim, S.A., Lei, M. (1987). Elastic constants and Debye temperature of polycrystalline $Y_1Ba_2Cu_3O_{7-x}$. Journal of Materials Research, 2(6): 786-789. https://doi.org/10.1557/jmr.1987.0786

[6] Block, S., Piermarini, G., Munro, R., Wong-Ng, W. (1987). The bulk modulus and Young's modulus of the superconductor $Ba_2CU_3YO_7$. Advanced Ceramic Materials, 2(3B): 601-605. https://cir.nii.ac.jp/crid/1360861291635273216#citations_container.

[7] Katagiri, K., Murakami, A., Kasaba, K. (2008). Evaluation of mechanical properties of high-temperature superconducting bulks fabricated by a melt-processing. Cryogenics, 48(3-4): 87-94. https://doi.org/10.1016/j.cryogenics.2008.02.003

[8] Rasih, N., Yahya, A. (2009). Effect of Ba-site substitution by Sr on ultrasonic velocity and electron-phonon coupling constant of DyBa2-xSrxCu3O7-δ superconductors. Journal of Alloys and Compounds, 480(2): 777-781. https://doi.org/10.1016/j.jallcom.2009.02.055

[9] Chakri, N., Benaldjia, A., Amara, A., Benloucif, M.R., Guerioune, M. (2007). Microscopic structural evolution in terms of porosity in high-Tc superconductors. Journal of Materials Science, 42(10): 3419-3424. https://doi.org/10.1007/s10853-006-1201-6

[10] Briggs, G.A.D. (2010). Acoustic Microscopy. Oxford University Press, Oxford.

[11] Tahraoui, T., Debboub, S., Boumaïza, Y., Boudour, A. (2012). Ultrasonic investigation for coated materials. International Journal of Microstructure and Materials Properties, 7(2/3): 254. https://doi.org/10.1504/ijmmp.2012.047504

[12] Tahraoui, T., Boumaïza, Y., Boudour, A. (2010). Ultrasonic study of the elastic properties of superconducting materials. Optoelectronics and Advanced Materials–Rapid Communications, 4(11): 1771-1774.
[13] Benbelghit, A., Boutassouna, D., Helifa, B., Lefkaier, I. (2006). Determination of the elastic properties of some coated materials by simulation of the analogue signal of the reflection acoustic microscope. NDT & E International, 39(1): 76-81. https://doi.org/10.1016/j.ndteint.2005.06.004
[14] Zinin, P.V., Weise, W. (2003). Theory and applications of acoustic microscopy. In Ultrasonic Nondestructive Evaluation: Engineering and Biological Material Characterization, pp. 653-724.
[15] Sheppard, C.J.R., Wilson, T. (1981). Effects of high angles of convergence on V(z) in the scanning acoustic microscope. Applied Physics Letters, 38(11): 858-859. https://doi.org/10.1063/1.92198
[16] Brekhovskikh, L.M., Godin, O.A., Palmer, D.R. (2000). Acoustics of layered media I: Plane and quasi-plane waves (Springer Series on Wave Phenomena Volume 5) Second, updated printing (Softcover); acoustics of layered media II: Point sources and bounded beams (Springer Series on Wave Phenomena Volume 10) Second, updated and enlarged edition. The Journal of the Acoustical Society of America, 107(4): 1809-1810. https://doi.org/10.1121/1.428553
[17] Phani, K.K. (2007). Correlation between ultrasonic shear wave velocity and Poisson's ratio for isotropic porous materials. Journal of Materials Science, 43(1): 316-323. https://doi.org/10.1007/s10853-007-2055-2.
[18] Asmani, M., Kermel, C., Leriche, A., Ourak, M. (2001). Influence of porosity on Young's modulus and Poisson's ratio in alumina ceramics. Journal of the European Ceramic Society, 21(8): 1081-1086. https://doi.org/10.1016/s0955-2219(00)00314-9
[19] Boccaccini, D.N., Boccaccini, A.R. (1997). Dependence of ultrasonic velocity on porosity and pore shape in sintered materials. Journal of Nondestructive Evaluation, 16(4): 187-192. https://doi.org/10.1023/a:1021891813782
[20] Phani, K.K., Niyogi, S.K. (1986). Porosity dependence of ultrasonic velocity and elastic modulus in sintered uranium dioxide–A discussion. Journal of Materials Science Letters, 5(4): 427-430. https://doi.org/10.1007/bf01672350
[21] Murthy, S.R. (2001). A study of ultrasonic velocity and attenuation on polycrystalline Ni-Zn ferrites. Bulletin of Materials Science, 24(6): 611-616. https://doi.org/10.1007/bf02704009
[22] Vasudev, B. (1995). Electrical and elastic properties of Mn-Zn ferrites. Ph.D. Thesis, Osmania University, Hyderabad.
[23] He, Y., Xiang, J., Jin, S., He, A., Zhang, J. (1990). Ultrasonic investigation of the layered perovskite ceramic superconducting systems. Physica B: Physics of Condensed Matter, 165: 1283-1284. https://doi.org/10.1016/S0921-4526(09)80227-5
[24] Almond, D.P., Lambson, E., Saunders, G.A., Hong, W. (1987). An ultrasonic study of the elastic properties of the normal and superconducting states of $YBa_2Cu_3O_{7-\delta}$. Journal of Physics F: Metal Physics, 17(9): L221-L224. https://doi.org/10.1088/0305-4608/17/9/007
[25] Cankurtaran, M., Saunders, G.A., Goretta, K.C., Poeppel, R.B. (1992). Ultrasonic determination of the elastic properties and their pressure and temperature dependences in very dense YBa2Cu3O7-x. Physical Review B, 46(2): 1157-1165. https://doi.org/10.1103/physrevb.46.1157
[26] Cankurtaran, M., Saunders, G.A., Goretta, K.C. (1994). Ultrasonic study of the temperature and pressure dependences of the elastic properties of fully oxygenated $YBa_2Cu_3O_{6.94}$. Superconductor Science and Technology, 7(1): 4-9. https://doi.org/10.1088/0953-2048/7/1/002
[27] Reddy, R., Prakash, O., Reddy, P. (1995). The effect of porosity on elastic moduli of YBa2Cu3O7-δ high Tc superconductors. Applied Superconductivity, 3(4): 215-222. https://doi.org/10.1016/0964-1807(95)00056-b
[28] Masi, L., Borchi, E., de Gennaro, S. (1996). Porosity behaviour of ultrasonic velocities in polycrystalline Y - B - C - O. Journal of Physics D: Applied Physics, 29(7): 2015-2019. https://doi.org/10.1088/0022-3727/29/7/039
[29] Ledbetter, H., Lei, M., Hermann, A., Sheng, Z. (1994). Low-temperature elastic constants of Y1Ba2Cu3O7. Physica C: Superconductivity, 225(3-4): 397-403. https://doi.org/10.1016/0921-4534(94)90741-2

NOMENCLATURE

E	Young's modulus, GPa
E_E	Relative Absolute Error of Young modulus, %
E_G	Relative Absolute Error of Shear modulus, %
E_K	Relative Absolute Error of Bulk modulus, %
E_{VL}	Relative Absolute Error of V_L, %
E_{VT}	Relative Absolute Error of V_T, %
FFT	Fast Fourier Transform
Frequency	f, MHz
G	Shear modulus, GPa
K	Bulk modulus, GPa
MAE	Mean absolute error
P	Pupil function
p	Porosity, %
R	Reflection coefficient
T	Temperature, K
Tc	Critical temperature
V	Velocity, m/s
V_L	Longitudinal velocity, m/s
V_{Liq}	Liquid velocity, m/s
V_T	Transverse velocity, m/s
V_R	Rayleigh velocity, m/s
V(z)	Curve signature, a.u
z	Distance, µm
Z_{Liq}	Liquid Impedance, MRy
Z_L	Longitudinal Impedance, MRy
Z_{Sol}	Solid Impedance, MRy
Z_T	Transverse Impedance, MRy

Greek symbols

θ	Incidence angle, °
θ_R	Rayleigh critical angle,°
Δ	Period, µm
ρ	Density, g/cm^3
ΔE	Absolute Error, m/s